FILE

INTERNAL DOCUMENT 178

I.O.S.

NEAR-SHORE TRIALS OF A FOUR-LEVEL SURFACE FOLLOWING CURRENT METER

G. Griffiths

NATURAL ENVIRONMENT RESEARCH COUNCIL

INSTITUTE OF OCEANOGRAPHIC SCIENCES

INSTITUTE OF OCEANOGRAPHIC SCIENCES

Wormley, Godalming,
Surrey GU8 5UB
(042-879-4141)

(Director: Dr. A. S. Laughton, FRS)

Bidston Observatory,
Birkenhead,
Merseyside L43 7RA
(051-653-8633)
(Assistant Director: Dr. D. E. Cartwright)

Crossway,
Taunton,
Somerset TA1 2DW
(0823-86211)
(Assistant Director: M. J. Tucker)

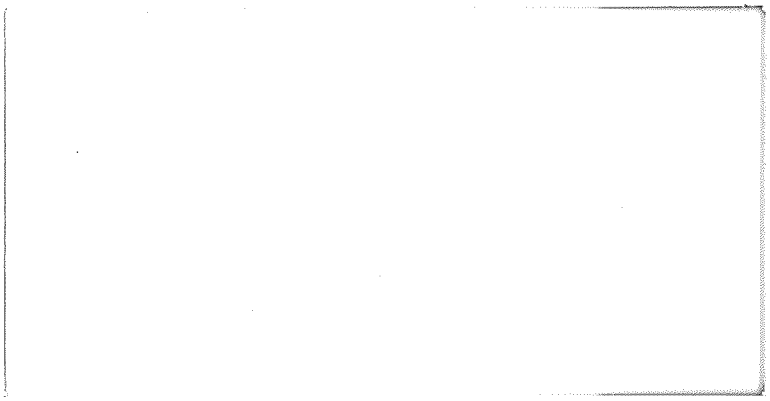

NEAR-SHORE TRIALS OF A FOUR-LEVEL SURFACE FOLLOWING CURRENT METER

G. Griffiths

INTERNAL DOCUMENT NO. 178

April 1983

Institute of Oceanographic Sciences,
Wormley, Godalming, Surrey GU8 5UB.

CONTENTS

NEAR-SHORE TRIALS OF A FOUR LEVEL SURFACE FOLLOWING CURRENT METER

1.0 INTRODUCTION

An intercomparison experiment was planned to take place in the Firth of Lorne near the SMBA site at Dunstaffnage in October 1982. Surface following electromagnetic current meters of two types were to be compared with an acoustic backscatter sonar, working off reflections from bubble clouds in the upper few metres (Thorpe & Hall, 1983). During September, however, the cable from the seabed acoustic transducers to the shore was damaged. The two types of e.m. current meters were deployed for an intercomparison and equipment trial.

The instruments used were the IOS vector averaging electromagnetic current meter (VAECM), equipped with an annular e.m. sensor, and a surface following Helmholtz type e.m. sensor at present under development. A map of the area of the experiment is shown in Fig. 1a, and the mooring positions and measurement depths in Fig. 1b.

Detailed results from the VAECM records will be given elsewhere; this report describes the multilevel sensor and its mooring arrangement, and gives an initial analysis of the data.

2.0 FOUR LEVEL SURFACE FOLLOWING CURRENT METER

The sensor is shown in Fig. 2a, and a block diagram of the electronics units in Fig. 2b. The instrument was designed to measure currents in the upper 0.4 m of the sea in the presence of waves. A thorough laboratory evaluation was undertaken of its response to both steady and wave-induced currents. Some of these results are given in Collar et al. (1983) in support of their theory of current measurement from a surface following sensor.

Signals from the two sets of orthogonal electrodes, at each of the four levels, were fed to a pre-amplifier. This was mounted on the upper crosspiece of the sensor. The arrangement was used to minimize the length of connecting leads carrying sub-microvolt signals. However, problems were encountered with this layout; these are examined in section 3.1.1. At the output of the current meter the filtered analogue signals were digitized by low power dual ramp ADC modules, as used in the IOS pitch roll buoy, at a rate of 8 Hz. After multiplexing the current meter data with the heading information from the compass, the data was telemetered ashore

through the conducting mooring cable. Power at 115V A.C. was fed to the buoy electronics from the shore units through the cable. Ashore, a line receiver and display unit allowed the data to be monitored, and a ¼" tape recorder logged the data.

2.1 Mooring configuration

The design of a suitable mooring is critical in the measurement of very near surface currents. As the multilevel sensor measures current to within 0.1 m of the sea surface, the following requirements must be met:

(i) the sensor should be perfectly exposed to the incident current and waves,

(ii) the sensor should be free to surface follow accurately while maintaining a steady heading. The steady heading was necessary because the compass was mounted on the mother buoy rather than on the sensor. Thus we assume the two buoys have the same heading.

These requirements led to the surface mooring design shown in Fig. 3. The sensor was attached via taut elastic cord to two outriggers. These outriggers were hinged onto plates clamped to a mother buoy. A canister on the mother buoy housed the electronics units and the compass was hung beneath a tripod clamped to the buoy plates. This arrangement allowed the sensor to move freely in heave, pitch and roll but restrained it in yaw. The mother buoy was loosely moored to the seabed, with a mooring cable length to water depth ratio of 1.3. This allowed it to surface follow and gave low cable tensions. The additional decoupling of the sensor (via the hinged outriggers and elastic cord suspension) served to improve the short wavelength surface following behaviour over a rigid arrangement. A fin was attached to the rear of the mother buoy in order to direct the sensor into the prevailing current. The geometry was such that deviations in alignment of up to $\pm 60^{\circ}$ could be tolerated before errors due to wake effects from the outrigger tubes would occur.

A "Y" bridle of plastic covered 6 mm wire rope was used to attach the mother buoy to an electrical and mechanical swivel at a depth of 5 m. A single electrical cable was attached to one arm of the bridle. The lower section of the swivel terminated the multiconductor armoured cable. This cable was used to moor the buoy and to telemeter the data ashore.

3.0 DATA RETURN AND QUALITY CHECKS

The data logging system which was used required tape changes every 3¼ hours (Runs 1 to 20) or every 2 hours (Runs 21-34), thus needing an operator. In all, the experiment provided more than 90 hours of data over nine days. The data logger tapes were translated to 9 track computer compatible tapes using a Camac system. On replay, the character error rate was about 1 in 10^5.

Table 1 gives a summary of the runs (note that Runs 24 to 30 were made with the sensor in the wake of the mother buoy). Calibration constants for offsets and sensitivity are given in Table 2. The data was edited in files of 1 hour duration (28800 scans), and linear interpolation was used to insert missing data. Short sections (10 minutes from each run) of data were examined using a program to calculate the kurtosis and skewness. No evidence of persistent problems was found for the current meter other than the occasional glitch. However, there was a high incidence of large kurtosis for the compass. This confirmed observations made during data recording that the compass channel suffered from drop-outs, especially during stormy conditions.

Edited data files were stored on the Honeywell computer under file names with the following convention:

GXG/IOS40/*/MLn-h

where * represents letters A through O, n represents the run number and h the hour number (1-4 for Runs 1-20, 1-3 for Runs 21-34). These data files were then stored on archive tapes, a list of the sub-catalogs and of the associated run numbers is given in Table 3.

Wind data for the period of the experiment was obtained from the met. station at SMBA, Fig. 4. An Aanderaa met. station was also used on a headland overlooking the moorings. However, premature battery failure and faulty wiring on the tape head reduced the period of good data to 4½ days.

3.1 Instrument performance

The sensor and electronics units worked well for the duration of the experiment in conditions ranging from flat calm to storm force 10 with 1.5 m waves.

3.1.1 Multilevel sensor

Zero drift occurred in three channels on or before deployment, and one other channel had drifted noticeably by Run 20. Due to the low sensitivity of the sensor and its large size, zero calibration in the laboratory was difficult. Errors of ±1 cm s^{-1} were expected in the zeros when the sensor was used at sea. The location of the pre-amplifier near the upper field coil demanded rigidity in its internal wiring in order to reduce inductive coupling through stray half turns. Some disturbance in the wiring could have caused changes in the zero offsets. Corrections to the offsets were made by assuming a smooth current change with depth on the axis aligned with the flow, and zero mean current on the axis across the flow. Several runs at different current speeds and directions under calm conditions were examined before the corrections were made. It is estimated that the errors in the corrections were ±1 cm s^{-1}. This error becomes a shear error of ±0.14, ±0.07, ±0.05 s^{-1} for 0.3 m, 0.2 m and 0.1 m measurements with reference to 0.4 m.

The sensor was recovered intact although four of the eight channels were subsequently found to be very noisy (several cm s^{-1} rms). No evidence for noisy behaviour on any channel was found during the experiment. Table 2 lists the pre- and post deployment offsets; an improvement in zero stability is clearly required.

3.1.2 Electronics units and data logging

No problems were encountered with the electronics units in the buoy or ashore. Data transmission through the swivel and conducting cable was perfect. There was some indication in the pattern of replay errors that the Camac software for translation was at times unable to handle the data rate when error printout was required.

3.1.3 Mooring configuration

The mooring survived the stormy conditions during the experiment, but on recovery, lock nuts on the eye bolts that coupled the large buoy to the wire mooring bridle were found to be loose. This was despite adequate torquing down and the application of "Locktite" thread locking compound. No damage was found to other mooring components.

The aligning fin failed to orient the sensor into the current for ~15% of the experiment; this was in one section from Run 24 to 30. The error was clearly seen in the data as similar values of current direction and buoy heading, normally the values would differ by 180°. Weather conditions were calm and the current speed exceeded 40 cm s^{-1} during part of this period.

During Run 30* the mooring was manually aligned into the current. The freeboard of the mother buoy was less than expected, and hence a larger fin area may be required for proper alignment.

The surface following action of the sensor was not inhibited by its attachment to the mother buoy. Spectra of currents taken during calm conditions showed two spurious responses near 0.33 Hz and 1 Hz (the natural frequency of the sensor itself). The 1 Hz component increased with depth amounting to a displacement of 0.02 m at the lower field coil. This suggests that, in the direction of the flow, the sensor was pitching slightly while pivoting about the surface buoyancy. The 0.33 Hz component which remained constant with depth suggests a lateral motion of the sensor, probably due to an oscillation of the whole surface buoy. Appendix 1 describes wave-tank experiments carried out to determine the cause.

The electrical swivel comprising a 0.5 m length of curled cable worked well. Nonetheless it should be noted that the tidal current vector at the site did not often rotate through 360°.

3.2 Results

As the data from the multilevel sensor was obtained in segments, techniques such as tidal analysis, low pass filtering and long period spectrum analysis could not be used. Initial evaluation of the data was made using the following methods:

(i) comparison of the stick plots of mean currents and current shear with respect to 0.4 m,

(ii) comparison of the east and north components of mean current and shear,

(iii) spectrum analysis over the band $\frac{1}{60}$ Hz to 4 Hz,

(iv) comparison with the VAECM at 1.2 m on mooring B,

(v) comparison with the wind data.

3.2.1 Mean currents

Currents vector averaged over 56¼ seconds were computed from the raw data to match the recording interval of the VAECMs. A high correlation was evident between the four levels at all times, for example, Run 16 is shown in Fig. 5. We estimate the relative accuracy of the mean currents to be better than ±1 cm s^{-1}.

*While servicing the flashing lights on the VAECM buoys.

The surface current at the site (Fig. 1) was dominated by the outflow of relatively fresh water from Loch Etive through the Falls of Lora. The data obtained from mooring B showed that the outflow reached this point on average 4.7 hours after high water at Oban, and persisted for about 5.6 hours. During the remaining part of the tidal cycle, the flow was much weaker from the quadrant south to west.

As a continuous record was obtained from the VAECM at B, low pass filtering was possible. This was done using a Lanczos weighting function digital filter of 95 coefficients with a cut-off period of 25 hours, working on half hourly samples of data (Fig. 6a). The same filter was applied to the SMBA wind data (Fig. 6b). A good correlation exists between the two records, note that the mean current to the west of about 18 cm s^{-1} is attributable to the Loch Etive outflow.

Results from the multilevel and VAECM sensors during two wind events are examined below. The choice of events for comparison was limited by the segmented multilevel data set.

During the southerly storm of day 301.5 to 302.5 a residual current of 16 cm s^{-1} to the north can be seen on the VAECM filtered record. Comparing the multilevel and VAECM records at this time (Fig. 7) shows a similar mean northward current for each instrument, though the VAECM showed a significantly larger westward current. This discrepancy can be attributed to the influence of the local topography on the outflow. The multilevel sensor mooring position was less exposed to direct flow from the Loch than the VAECM (Fig. 1b).

During the period from day 305.5 to 306.0, the wind increased rapidly to 8 m s^{-1} from a flat calm whilst veering from south east to west. At the VAECM mooring B this produced a strong 30 cm s^{-1} flow to the east into the Loch (Fig. 8). The filtered VAECM record shows this as a residual current of about 2 cm s^{-1} to the east (Fig. 6a). However, the multilevel sensor showed a current to the north east, parallel to the coast (Fig. 8). This suggests the possibility that the eastward current generated in the Firth was deflected to the north east by the shoreline whereas mooring B had open water to the east (Fig. 1b).

The complex currents in the area, together with a lack of measurements by other means, preclude a determination of the absolute accuracy of the currents measured by the multilevel sensor. In terms of general behaviour

and order of magnitude, however, they do agree with the acoustic backscatter measurements detailed in Thorpe and Hall (1983). There was no evidence for rectification of orbital motion by the sensor.

3.2.2 Measurement of shear

At the site of the experiment two mechanisms for the generation of shear were present; surface wind stress and fresh water outflow.

During the experiment the wind speed reached 15 m s^{-1} from the south west, with a fetch of over 20 km. Assuming a logarithmic boundary layer near the surface as in Shemdin (1972),

$$(u_{z_1} - u_{z_2}) = \frac{u^*}{\kappa} (\ln \frac{z_2}{z_1}) \qquad (1)$$

κ = Von Kármán constant = 0.4

where $u^* = 1.56\ W_\infty \times 10^{-3}$. W_∞ = free field wind speed.

Using $z_1 = 0.1$ m, $z_2 = 0.4$ m and $W_\infty = 15$ m s^{-1} we would thus expect a shear of 0.27 s^{-1}.

The other mechanism for shear generation arises from the fresh water outflow from Loch Etive. A strong density gradient of about 1.8 kg m^{-4} existed in the upper 3 m under calm conditions as detailed in Thorpe (1982). This gradient would be capable of supporting considerable shear.

3.2.3 Shear measurements during calm conditions

During days 303 and 306, there were periods when the wind speed was very low (<3 m s^{-1}) for several hours. These periods coincided with the outflow from the Loch. Records were obtained from a time lapse cine camera located on a headland overlooking the mooring site. Fronts were visible on the sea surface during these times as colour changes, and were clearly recorded by the camera.

Fig. 9 shows the shear with respect to the 0.4 m level for the east and north components during day 303. A large increase in shear coincides with the change in mean current direction, from west to south west, just after 1200 hours. This shear persisted for the rest of the day. A further peak to 0.6 s^{-1} occurred near 1400 hours. The records from 0.1 m and 0.2 m were very similar, but a systematic error is suspected for 0.3 m.

An estimate of the shear sustainable in a given density gradient can be made using the gradient Richardson number,

$$Ri = \frac{g(\partial\rho/\partial z)/\rho}{(\partial u/\partial z)^2} \qquad (2)$$

where ρ = density, g = gravity and u = horizontal velocity. The Miles-Howard

theorem (Miles (1961) and Howard (1961)) predicts flow stability for a Richardson number greater than 0.25.

If we assume a density gradient 1.8 kg m^{-4} under calm conditions, then equation 2 predicts a shear of 0.27 s^{-1} at the critical Richardson number of 0.25. This value of shear is similar to the long term shear seen in Fig. 9. The consistency between the predicted and measured values shows that the multilevel sensor is capable of shear measurement in the upper 0.4 m of the sea.

The same general behaviour of the outflow shear can be seen during day 306 (Fig. 10). The major component of the shear following the passage of the front during day 303 was to the east, whereas during day 306 the shear was to the north. As the shears calculated from the upper three layers were very similar, a linear velocity gradient over the upper 0.4 m is implied.

The steps in the shear time series were associated with the passage of fronts at the buoy as recorded by the camera. Such events are shown in Figs. 9 and 10.

3.2.4 Shear measurements during stormy conditions

A scatter plot of the shear between 0.1 m and 0.4 m against wind speed is shown in Fig. 11. The entire current data set is represented at half hourly intervals to coincide with wind speed measurements. A clear tendency towards strong shear at times of low wind speed is seen, with some indication of shear into the wind at the higher wind speeds. This suggests that the predominant mechanism for the generation and support of near surface shear at this site was the density gradient arising from the fresh water outflow of Loch Etive. The importance of zero offsets in the current meter increases as the shear reduces, thus care must be taken in the interpretation of the smaller shears measured under stormy conditions.

Some evidence for a shear less than that predicted by a logarithmic boundary layer, equation 1, can be obtained from both the VAECM and multilevel sensors.

Examination of the VAECM filtered record (Fig. 6a) shows the northward wind driven current to be between 2% and 3% of the wind speed. If a logarithmic profile is assumed,

$$(u_o - u_z) = \frac{u^*}{\kappa} \cdot \ln\left(\frac{z}{z_{ow}}\right) \qquad (3)$$

with $u^* = 1.56\ W_\infty \times 10^{-3}$ as before and $z_{ow} = 3.4 \times 10^{-4}$ m (from the results of Shemdin (1972) at W = 9.1 m s^{-1}), then the required surface velocity would be between 5.2% and 6.2% of the wind speed. These are higher than published values (Huang, 1979), which tend to cluster around 3%.

The multilevel sensor gave six hours of data on day 314 during a south westerly gale which prevented recovery of the moorings. The wind speed was from 12 to 15 m s^{-1} and wave heights were visually estimated to be 1.5 m. The shear (Fig. 12) was about 0.08 s^{-1} to the west, and about 0.14 s^{-1} to the south. The resultant of 0.16 s^{-1}, with an error margin of ±.05 s^{-1} (for the 0.1 m-0.4 m measurement), is significantly less than the value of 0.27 s^{-1} predicted for a logarithmic boundary layer as calculated in section 3.2.2. An increase in zero calibration accuracy to ±1 mm s^{-1} would be necessary before the sensor could be used for detailed measurements of near surface shear.

4.0 FUTURE DEVELOPMENT

The following have been identified as areas for improvement and further development:

(a) Sensor

(i) The pre-amplifier position created problems as outlined in section 3.1. It should either be incorporated in the main electronics housing and great care taken with signal leads and connectors, or enclosed in a magnetic shield, e.g. mu-metal box.

(ii) The zero stability must be improved, partly through (i) above, and consideration should be given to an in-situ zero calibration.

(iii) Some additional damping of the sensor's natural pitch period is required, it may also be possible to decrease the period.

(b) Electronics

(i) A vector averaging package is under construction which will allow the instrument to sample continuously and yet be self-contained.

(c) Mooring

(i) Mooring components and techniques should be uprated for exposed sites. All nuts and shackles which are subjected to vibration near the surface should be better seized.

(ii) The dynamics of the rubber cord suspension should be examined to determine its natural period. Methods of damping and or stiffening should then be devised.

(d) General

It would be of advantage in shear studies if a temperature measurement could be made at each of the four levels. A resolution and accuracy of better than .005^{o}C would be required to match a current meter accuracy of 1 mm/s under conditions such as those seen at the Dunstaffnage site.

5.0 CONCLUSIONS

The experiment has shown the feasibility of current measurement very close to the sea surface using a multilevel electromagnetic current sensor.

Mean currents were measured to an estimated accuracy of ±1 cm s^{-1} under all sea surface conditions, with high correlation between the four levels. A major objective of the sensor design, i.e. measurement of near surface shear, has been achieved, though not to the accuracy required for detailed comparison with theories of near surface flow. A stable zero calibration to within ±1 mm s^{-1} would be required to resolve a logarithmic boundary layer, generated by a 6 m s^{-1} wind, to within ±20%. We thus require an order of magnitude improvement in the zero calibration of the sensor.

The most easily understood shear measured was sustained by a density gradient rather than wind stress. Further analysis of the data set may yield more information on the wind driven flow.

Weaknesses in the design of the sensor, electronics units and mooring configuration have been identified and courses of action and further development suggested.

6.0 ACKNOWLEDGEMENTS

The experiment could not have succeeded without the assistance of P.G. Collar, C.H. Clayson, V.A. Lawford, A.J. Bunting, C.A. Hunter and J.R. Perrett. Construction and maintenance of the sensor was by A.C. Braithwaite. The help of the master and crew of R.V. Calanus and the SMBA diving team is gratefully acknowledged.

7.0 REFERENCES

Collar, P.G., R.M. Carson and G. Griffiths (1983) Measurement of near-surface current from a moored wave-slope follower. Deep-Sea Research, 30(1), 63-75.

Howard, L.N. (1961) Note on a paper by John W. Miles. J. Fluid Mechanics, 4, 509-512.

Huang, N.E. (1979) On surface drift currents in the ocean. J. Fluid Mechanics, 91(1), 191-208.

Miles, J.W. (1961) On the stability of heterogeneous shear flows. J. Fluid Mechanics, 91(1), 496-508.

Shemdin, O.H. (1972) Wind-generated current and phase speed of wind waves. J. Physical Oceanography, 2(4), 411-417.

Thorpe, S.A. (1982) On the clouds of bubbles formed by breaking wind waves in deep water, and their role in air-sea gas transfer. Phil. Trans. R. Soc., A 304, 155-251.

Thorpe, S.A. and A.J. Hall (1983) The characteristics of breaking waves, bubble clouds, and near surface currents observed using side-scan sonar. Continental Shelf Research, 1(4), to appear.

Appendix 1

A laboratory investigation of the natural period motion of the multilevel sensor

Section 3.1.3 discussed the presence of a spurious response near the natural pitch period of the sensor. A laboratory investigation was made in an attempt to repeat the observed response, hence to discover its cause and suggest modifications to the sensor and or suspension.

As the surface mooring components used at sea could not be accommodated in the wavetank, a simpler arrangement was used. This consisted of two dexion outriggers clamped to the platform beneath the carriage. The same elastic cord as was used at sea coupled the sensor to the outriggers. Any effects due to the hinged outrigger tubes and the mother buoy were thus removed.

Tests were made in waves of various periods and also under steady tow. Fig. A1 shows the spectra obtained under steady tows of 10 cm s^{-1} and 42 cm s^{-1}. In both cases, peaks at ~1 Hz and ~0.5 Hz are present. The energy levels at frequencies were much lower than those observed at sea.

Table A1 summarises the energy levels found at 1 Hz in the wavetank and at sea. We were unable to use longer wavelengths because the second harmonic of the wave frequency then intruded into the band of interest around 1 Hz.

Table A1 Energy levels at 0.4 m in the wavetank and at sea

Wavetank		
0.75 s waves	< .096 cm^2/s^2	
1.45 s waves	< .482 cm^2/s^2	
42 cm s^{-1} tow	≈ .024 cm^2/s^2	
10 cm s^{-1} tow	≈ .049 cm^2/s^2	
At rest	≈ .009 cm^2/s^2	
At Sea		**Surface Conditions**
Run 8	≈ 5.0 cm^2/s^2	Flat calm, strong current.
Run 16	≈ 3.6 cm^2/s^2	Calm, current variable.
Run 23	≈ 4.8 cm^2/s^2	Flat calm, strong current.
Run 33	≈ 6.2 cm^2/s^2	Heavy seas.

We have shown that the sensor is liable to give a strong output at its natural pitch frequency even under steady wavetank conditions. However, as the energy levels observed were much lower in the laboratory, the surface mooring components must have provided a significant part of the driving force. An increase in the natural frequency would be obtained if the reserve buoyancy of the sensor could be increased. This would then enable a simple low pass filter to be used to remove the spurious oscillation. The introduction of dampling plates would be likely to interfere with either the flow around the sensor or its surface following ability.

There is no evidence in either the near-shore experiment or the laboratory study to indicate an error in mean flow measurement arising from the oscillations at the natural frequency.

Appendix 2

HONEYWELL FILES FOR MULTILEVEL SENSOR DATA ANALYSIS

These programs and data files are archived under the relevant subcatalogs:

1. Data entry from tape, and error checking

/OBAN/CAMAC*	- reads data in 1 hr blocks and saves onto disk.
/ERROR	- CRUN file - runs /OBAN/JCLCAMER* which calls /OBAN/CAMER checks for error indicators.

2. Calibration, shear calculation and plotting

/CAL	- CRUN file - runs /OBAN/DATACAL calibrates data to cm s^{-1} East and North.
/TIME	- CRUN file - runs /OBAN/TIMECAL puts timebase onto calibrated file.
/SHEAR	- CRUN file - runs /OBAN/SHEARCAL calculates shear.
/PLOT	- CRUN file - runs /OBAN/FEAPL plots feather plots of mean data.
/SPLOT	- CRUN file - runs /OBAN/SHEARFPL plots feather plots of shear data.
/STATS	- CRUN file - runs /OBAN/JCST* uses files of J.A. Ewing for statistics of raw data.

3. Miscellaneous computations

/OBAN/PROC/SHEARPLT	- plots shear as East, North.
/OBAN/PROC/SDCAL	- calculates standard deviation of calibrated data.
/OBAN/PROC/SDPLT	- plots s.d. data.
/OBAN/PROC/ZCPCAL	- calculates zero crossing period of calibrated data.
/ANALYSIS/OBANFFT	- calculates spectra from 1 hour of calibrated data.
/ANALYSIS/OBANFFTP	- plots spectra.
/ANALYSIS/ORBIT	- calculates VP-VCM from Collar et al. (1983).
/ANALYSIS/FILTDES	- design of digital filters.

*Runs in batch mode.

Table 1

Summary of Times and Comments for ML Sensor Experiment, Oban 1982

Run	Date	T Start	Comments
1	28-10-82	301.7859	Calming down
2		.9229	Calm at start of tape
3	29-10-82	302.3498	Strong S wind throughout tape
4		.4920	"
5		.6408	Continuing strong wind
6		.7859	Calming down
7		.9281	
8	30-10-82	303.4024	Flat calm
9		.5419	Wind increasing from E surface calm
10		.7669	Freshening S.E. wind
11	31-10-82	304.4230	Slight W swell, wind from S
12		.5672	Wind freshening SW breakers
13		.7076	Westerly wind larger waves
14		.8586	
15		.9979	
16	1-11-82	305.5317	Calm rippled
17		.6845	NW wind freshening, whitecaps
18		.8223	Wind decreased sea calmer
19	2-11-82	306.3345	Calm low waves some swell
20		.4737	Calmer low swell very little waves
21		.6119	Light airs very low swell rippled
22		.7002	Glassy smooth patches
23		.7896	
24	3-11-82	307.3477	Calm rippled)
25		.4358	)
26		.5240	)
27		.6062	) !Sensor in buoy wake!
28		.6951	)
29		.7832	)
30	4-11-82	308.3451	No wind rippled sea no swell
31		.4624	Calm light airs
32	10-11-82	314.4690	Heavy seas
33		.5465	"
34		.7215	"

Table 2 Calibration Constants and Offsets

Ch No	Sensitivity (cm/s /digit)	Offsets Used (Digits) Pre	Post
1	+.278	513 513	Noisy
2	-.278	493 493	488
3	-.299	513 480	Noisy
4	+.300	466 437	Noisy
5	+.303	542 542	524
6	-.294	548 548	535
7	-.270	488 440	469
8	-.256	547 547 (565 after Run 20)	Noisy

Table 3 Data catalogs and associated run numbers

GXG/IOS40/A	Runs 10,11
GXG/IOS40/B	Runs 9,13
GXG/IOS40/C	Runs 19,20
GXG/IOS40/D	Runs 23,24,25
GXG/IOS40/E	Runs 14,32
GXG/IOS40/F	Runs 15,16
GXG/IOS40/G	Runs 17,18
GXG/IOS40/H	Runs 21,22,30
GXG/IOS40/I	Runs 26,31,34
GXG/IOS40/J	Runs 3,33
GXG/IOS40/K	Runs 27,28,29
GXG/IOS40/L	Runs 2,4
GXG/IOS40/M	Runs 8,12
GXG/IOS40/N	Runs 5,7
GXG/IOS40/O	Runs 1,6

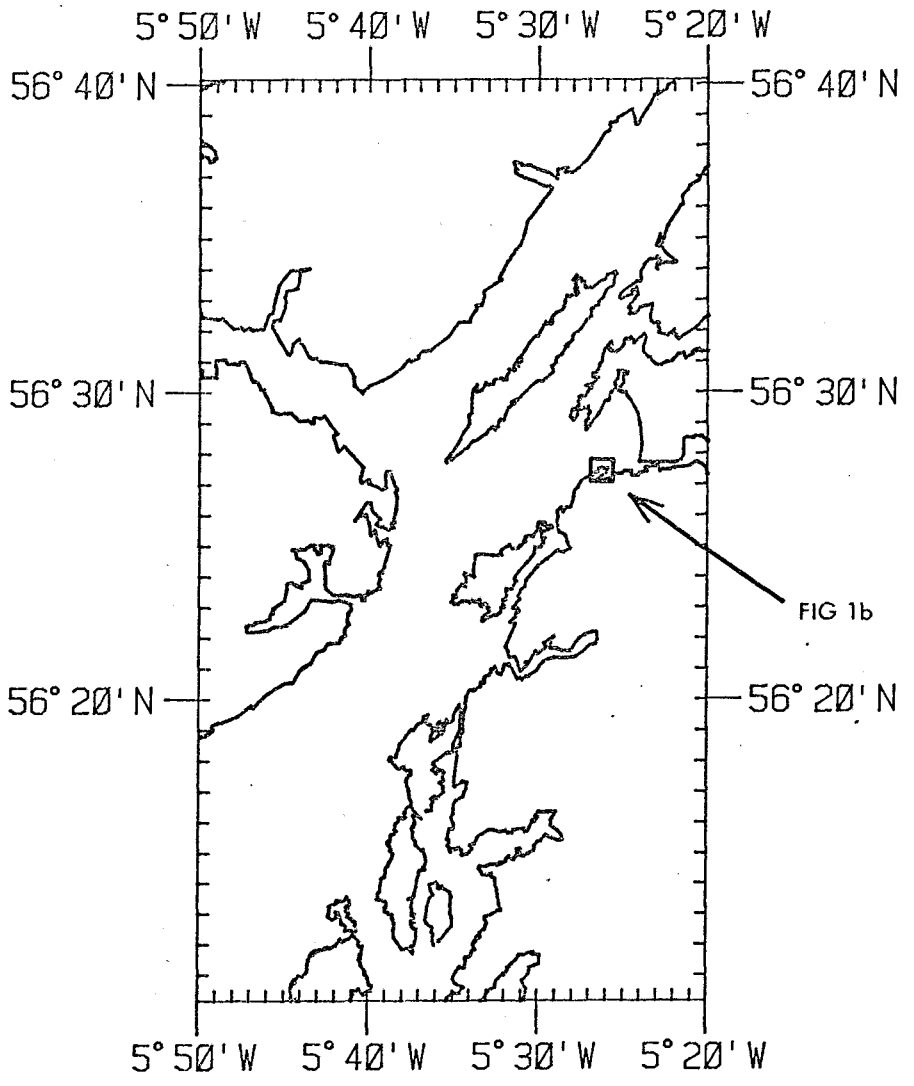

Fig. 1(a) Experiment area in the Firth of Lorne.

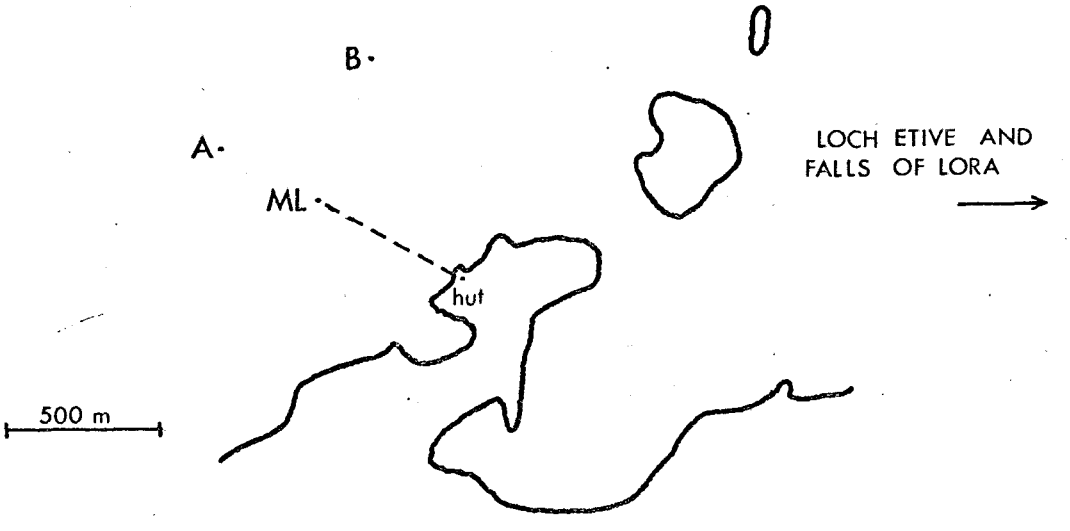

Fig. 1(b) Mooring positions. (Mean water depth ~32 m).
Mooring A = VAECM 3 at 0.5 m, VAECM 4 at 0.5 m,
B = VAECM 10 at 0.5 m, VAECM 11 at 1.2 m,
ML = Multilevel Sensor at 0.1, 0.2, 0.3 and 0.4 m.

Fig. 2(a) The Multilevel Sensor.

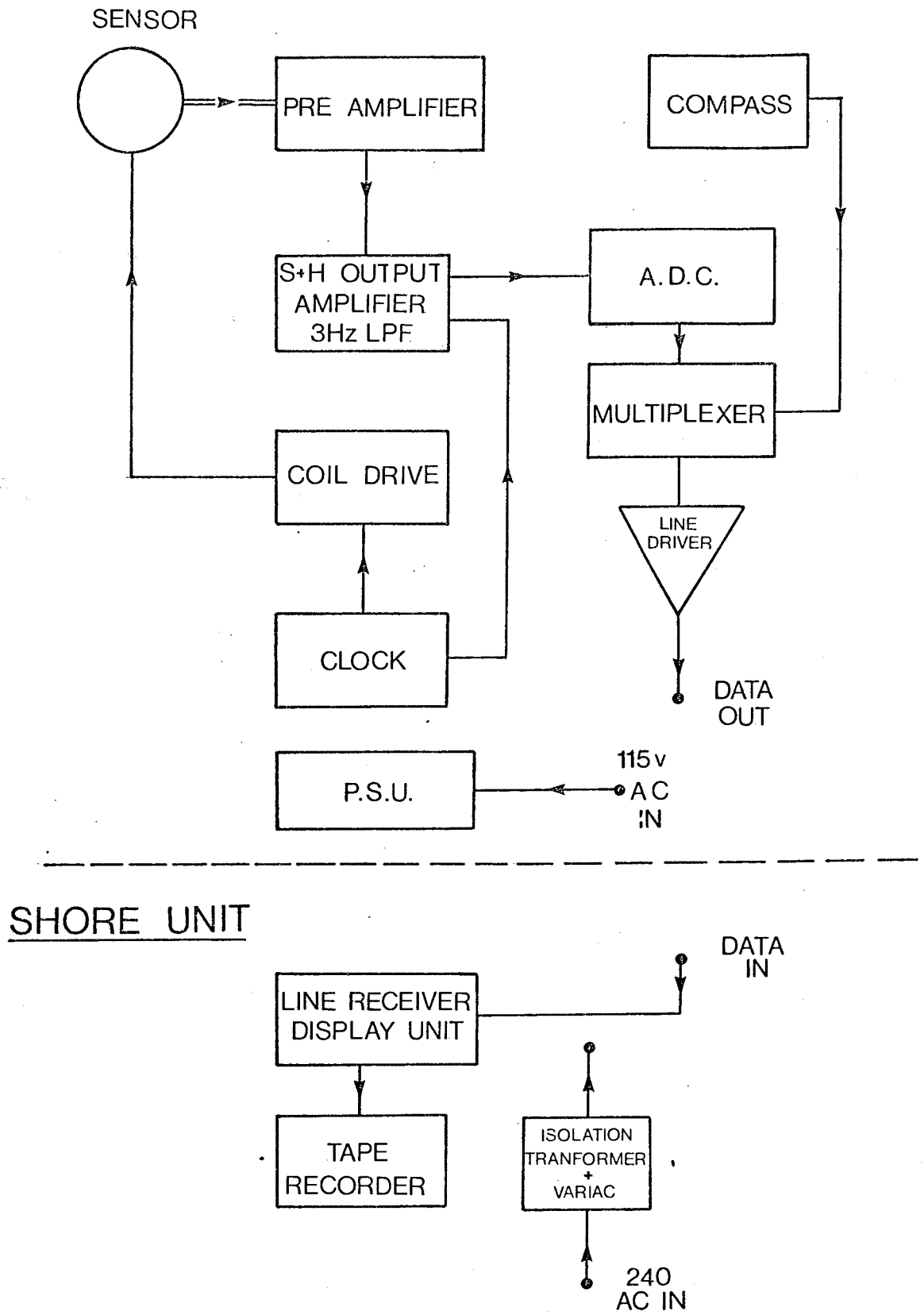

Fig. 2(b) Block diagram of the electronics units.

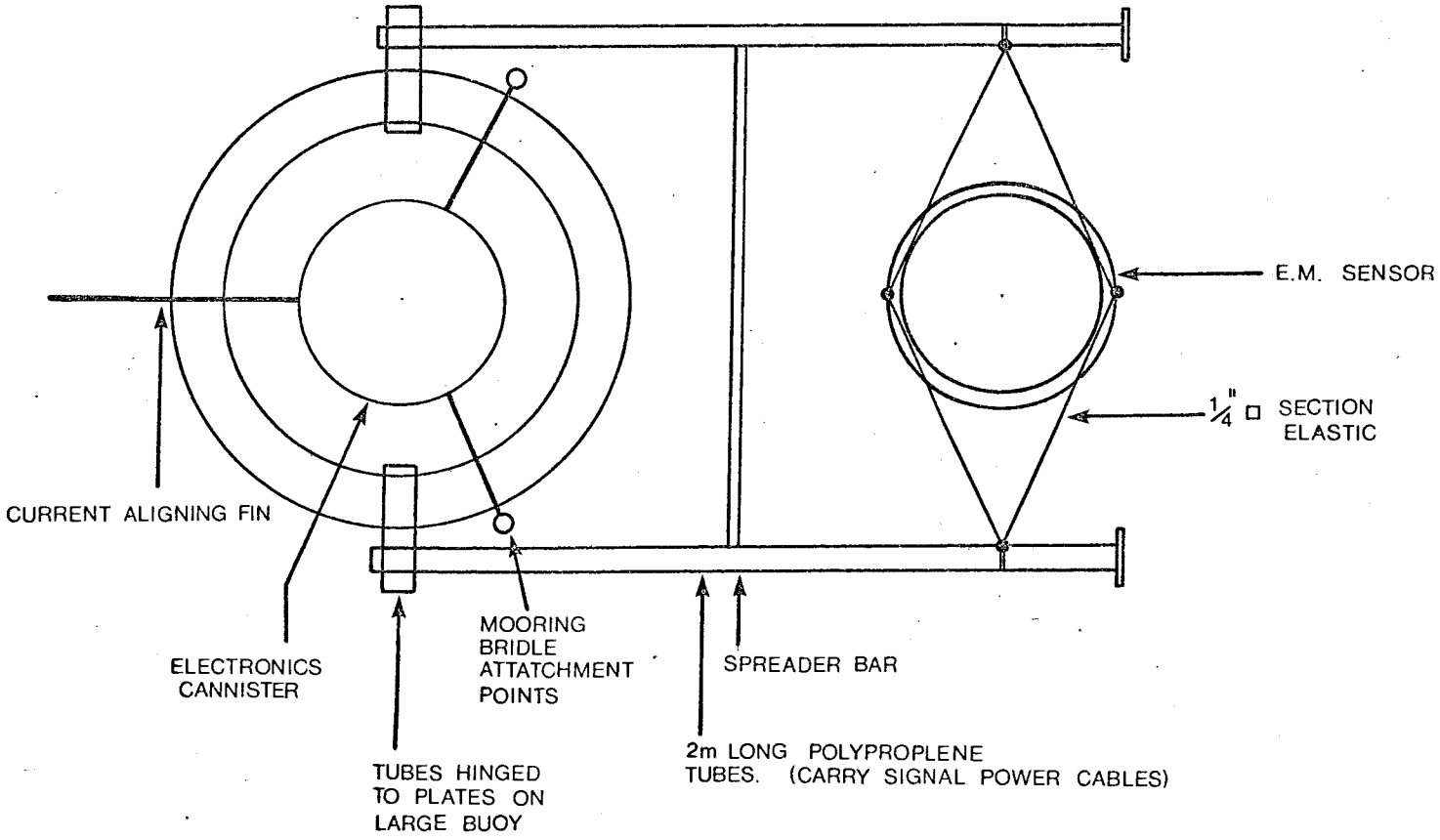

Fig. 3 Components of the surface mooring.

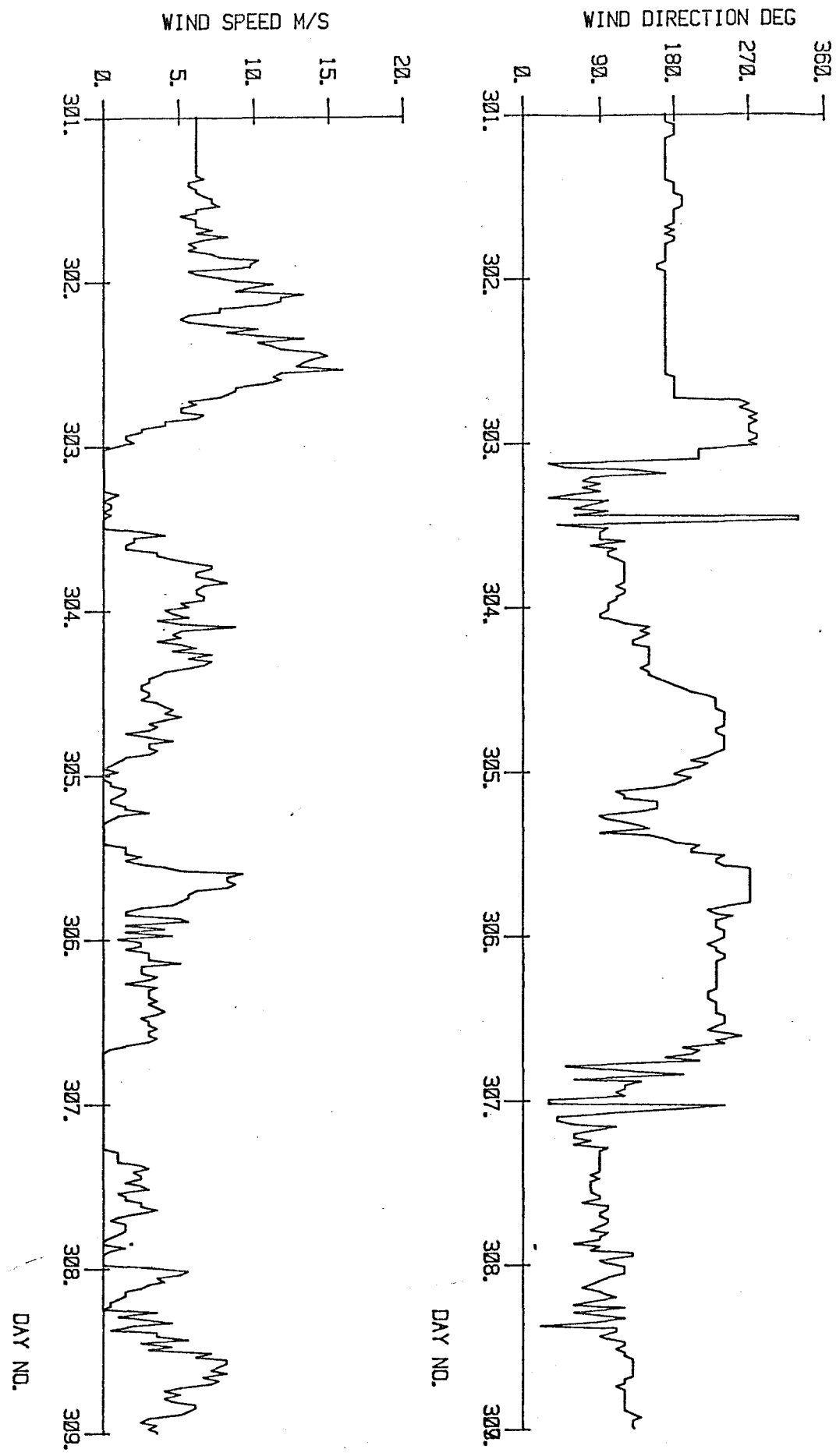

Fig. 4 Wind speed and direction from the SMBA met. station.

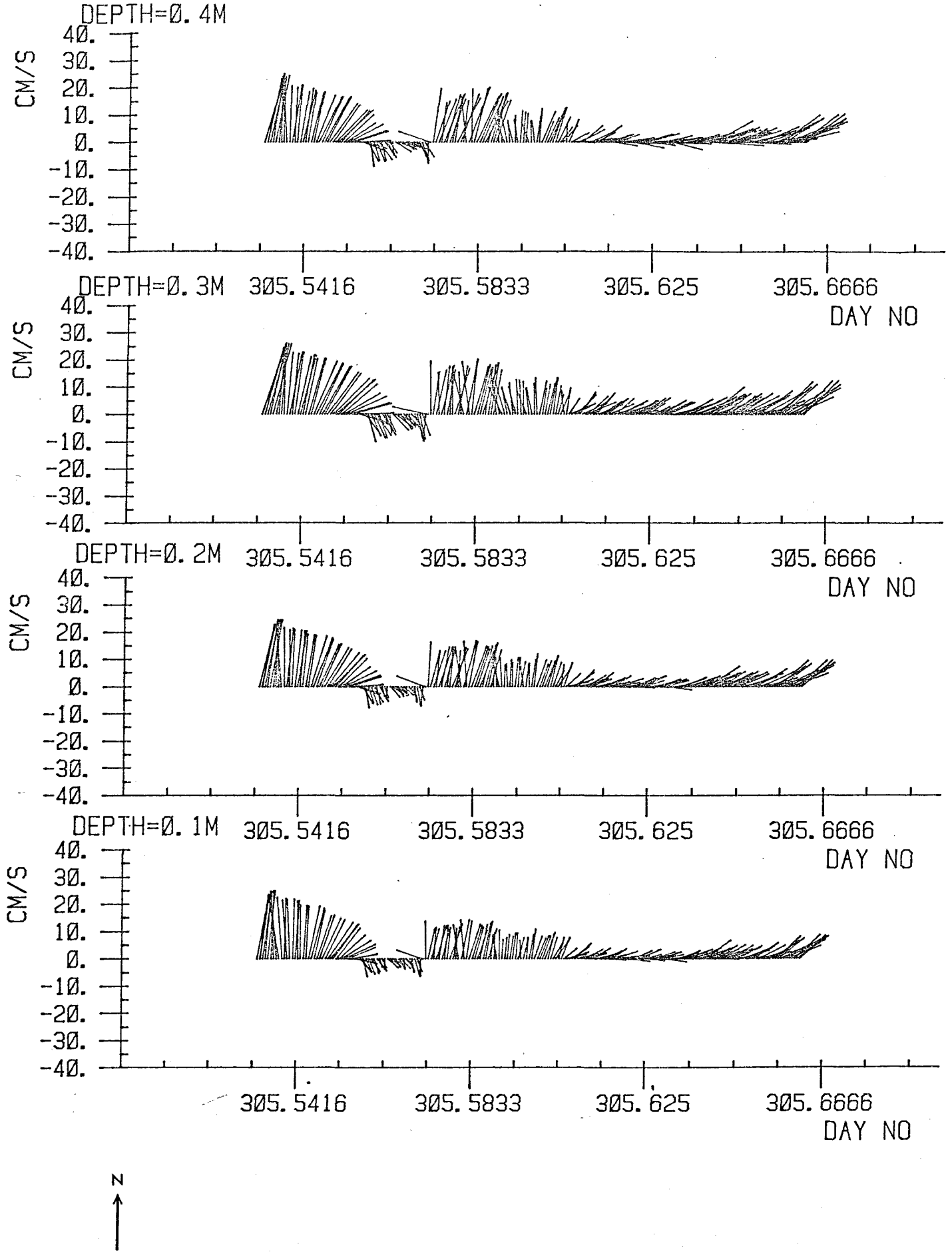

Fig. 5 Stick plots of mean current from run 16.

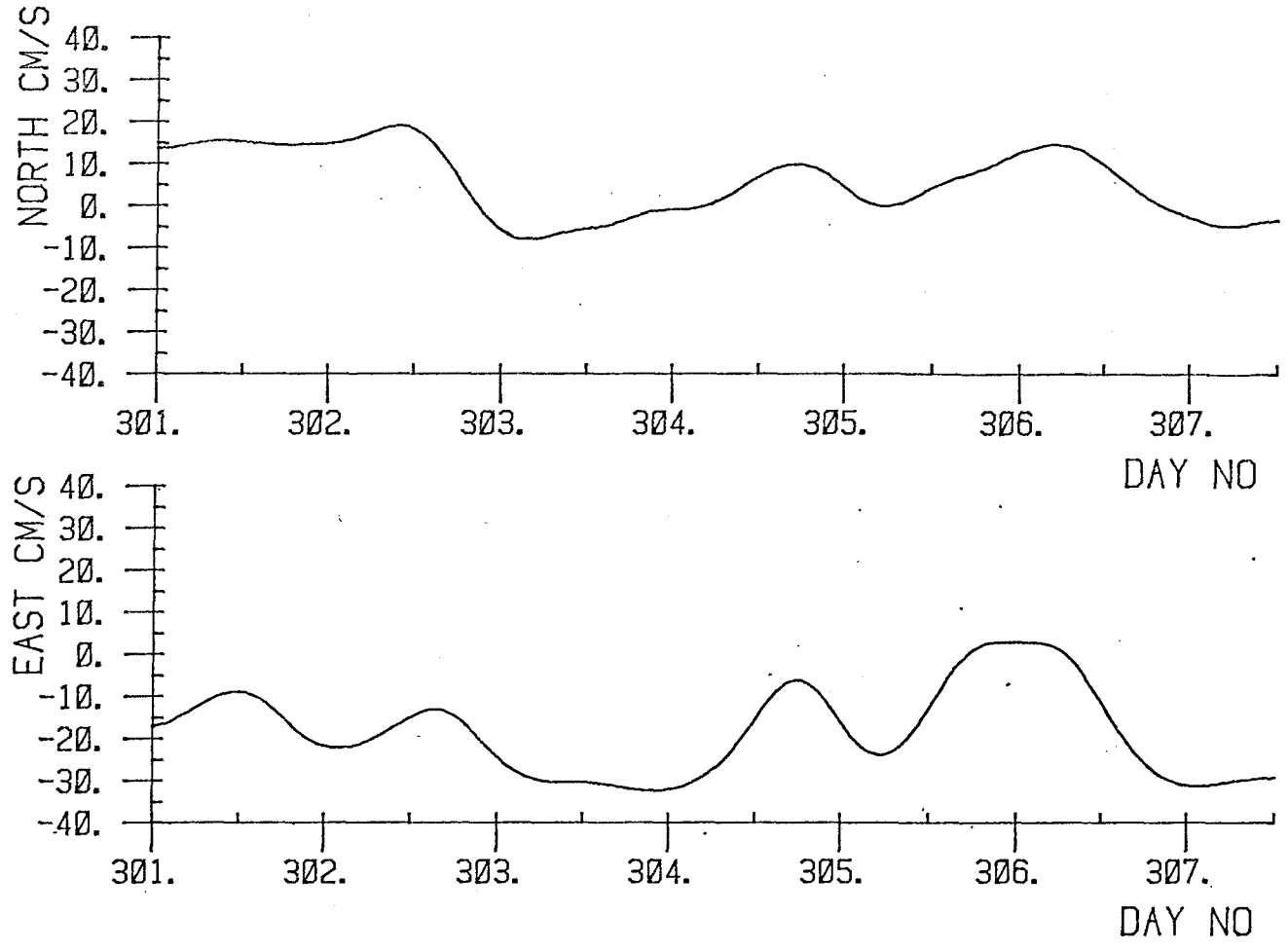

Fig. 6(a) Low pass filtered VAECM 11.

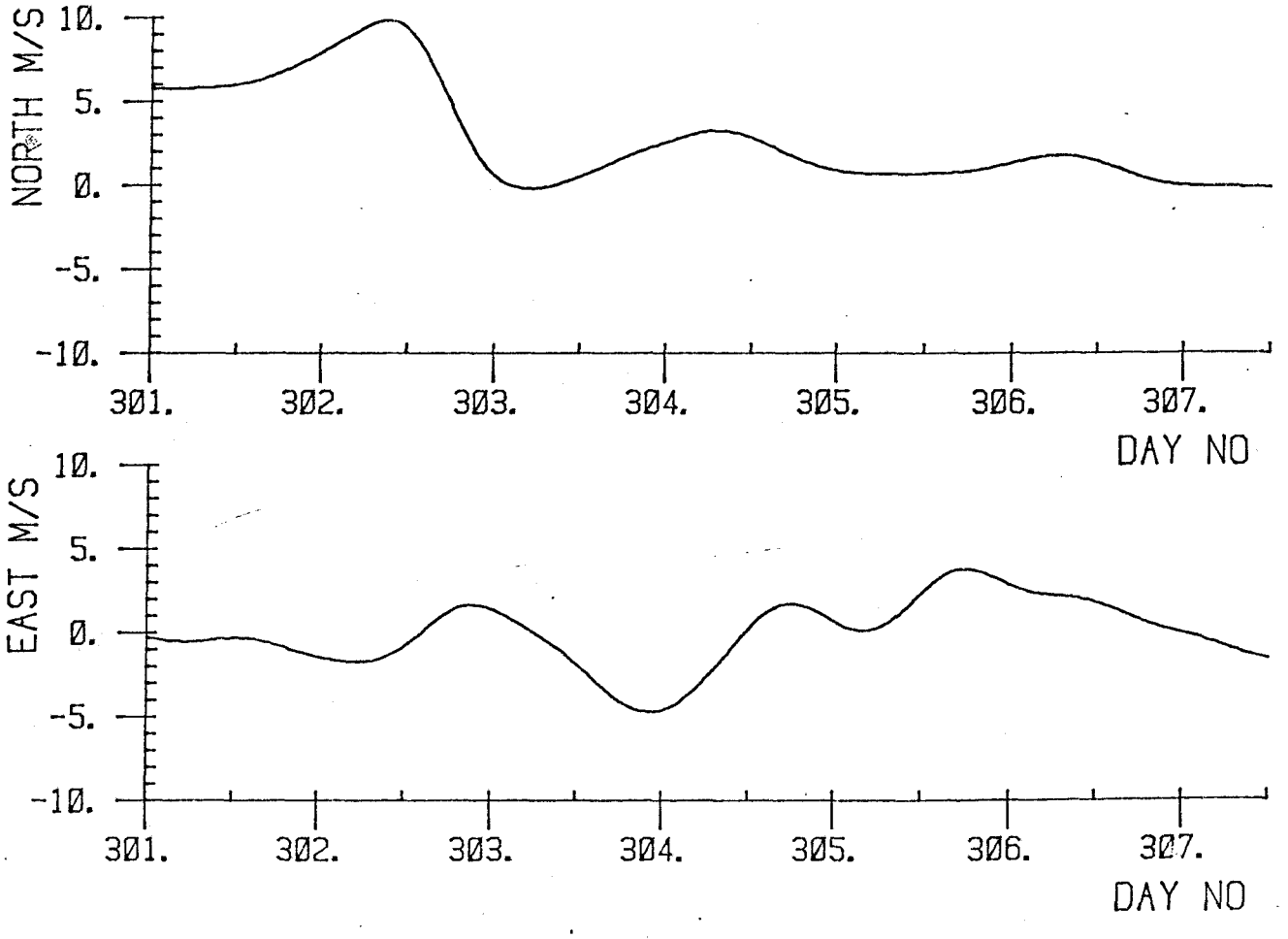

Fig. 6(b) Low pass filtered wind data.

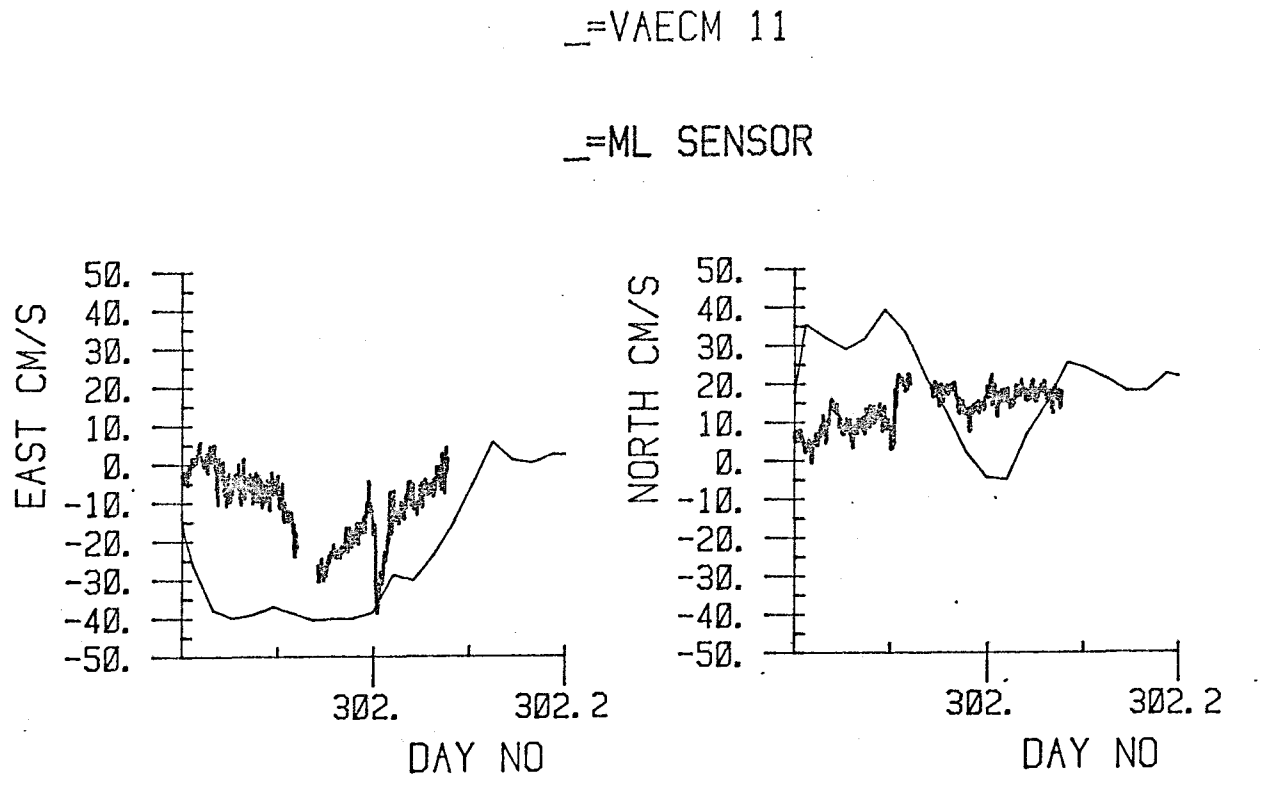

Fig. 7 Mean east and north currents for the multilevel and VAECM from runs 1 and 2.

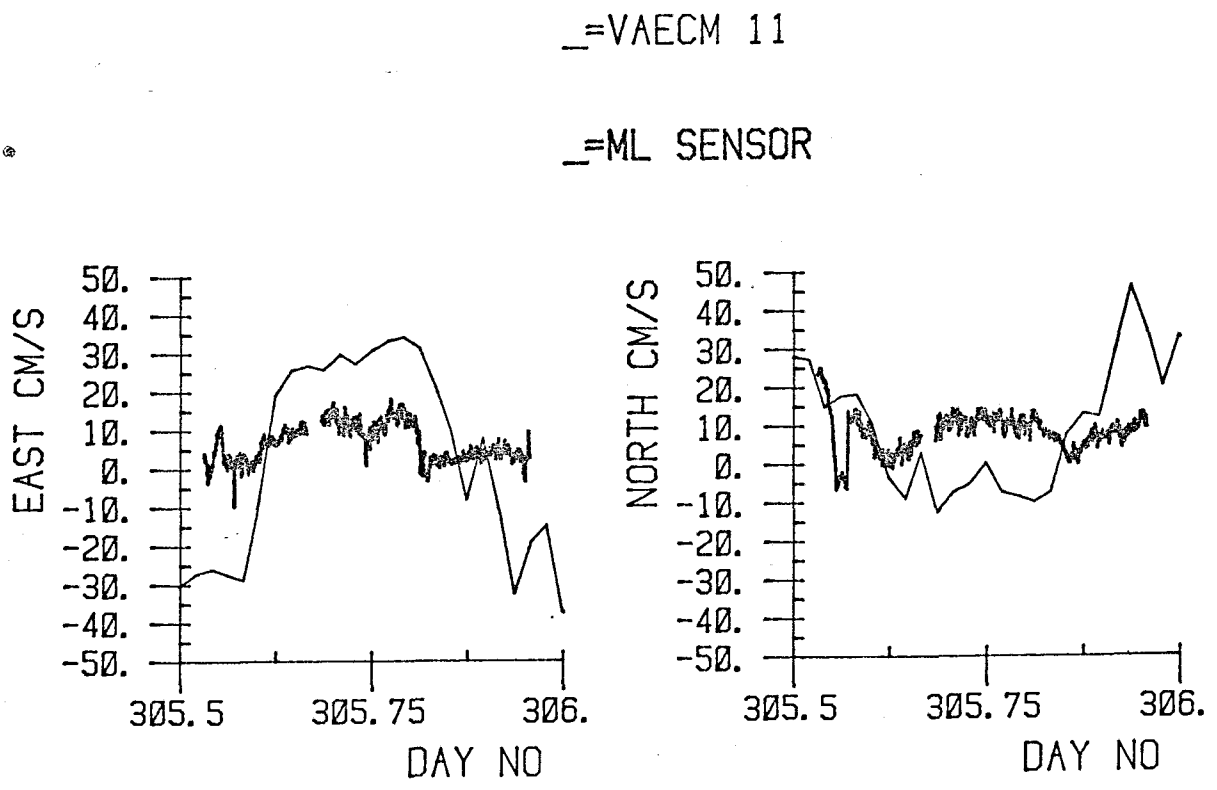

Fig. 8 Mean east and north currents for the multilevel and VAECM for day 305.

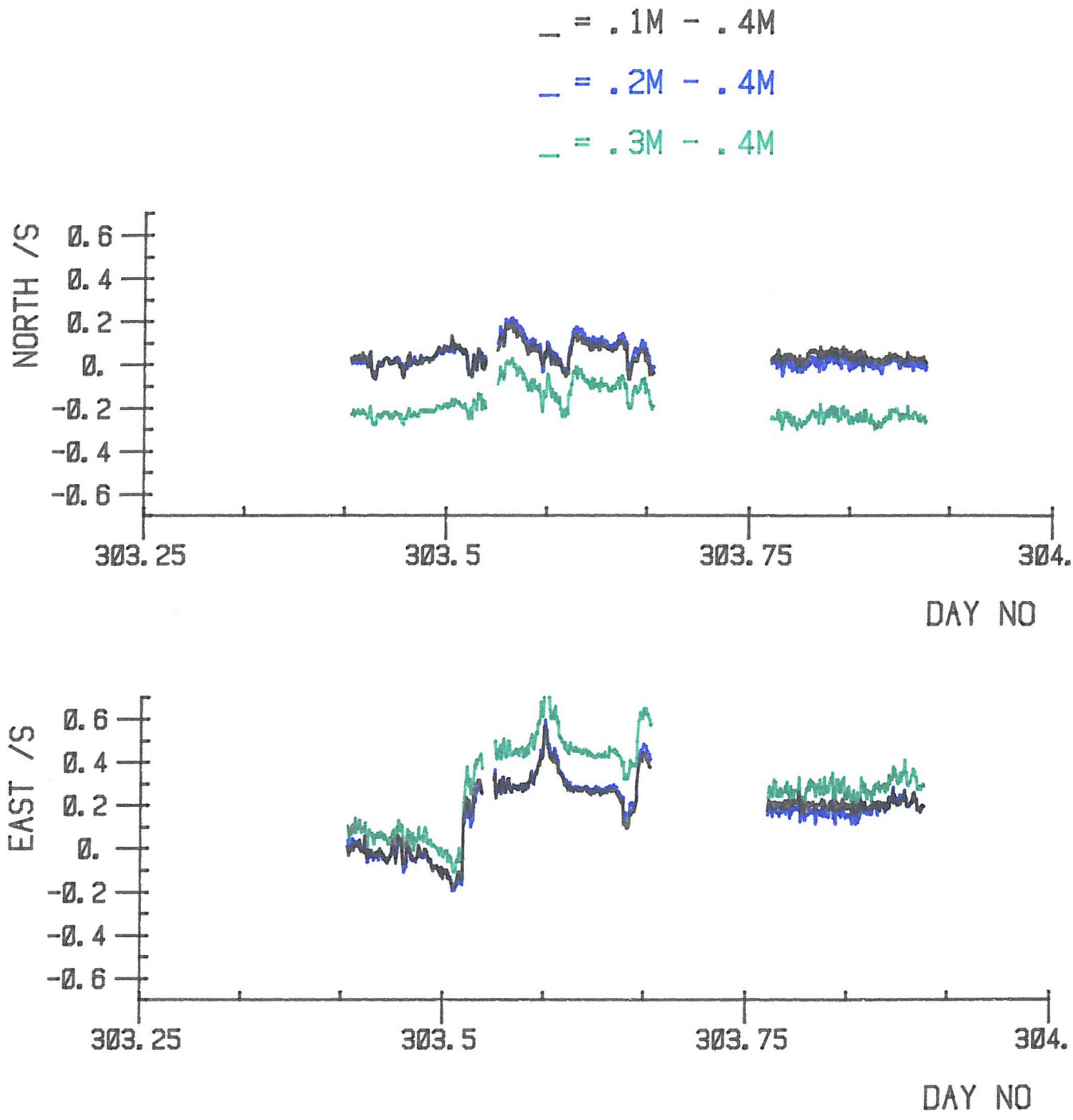

Fig. 9 Shear from the multilevel sensor for day 303. Fronts identified from film taken at these times.

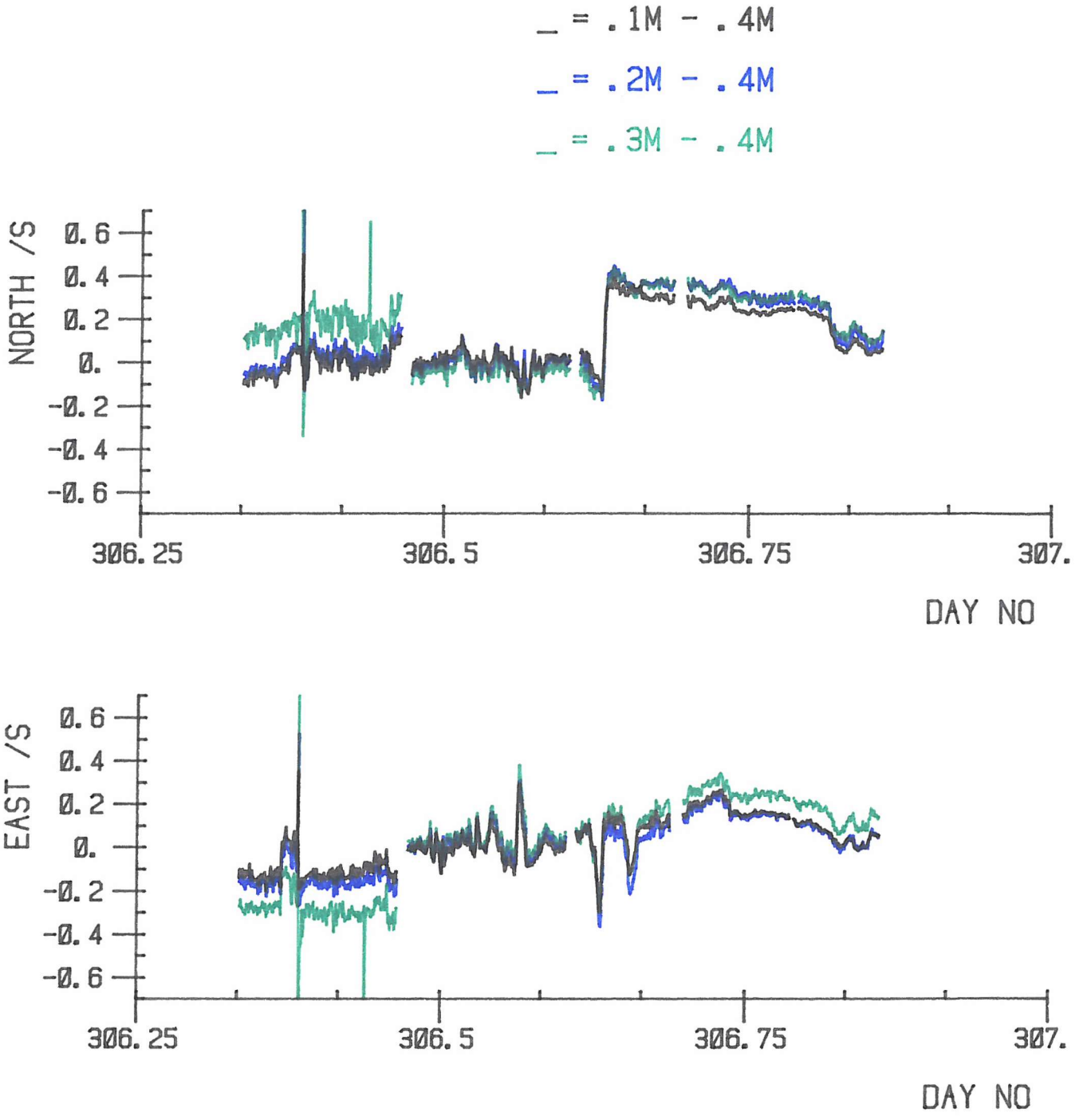

Fig. 10 Shear from the multilevel sensor for day 306.
NOTE: The sudden change in .3m-.4m data is due to the change in zero offset for channel 8 used in the computation See section 3.1.1 and table 2.

Fronts identified from film taken at these times

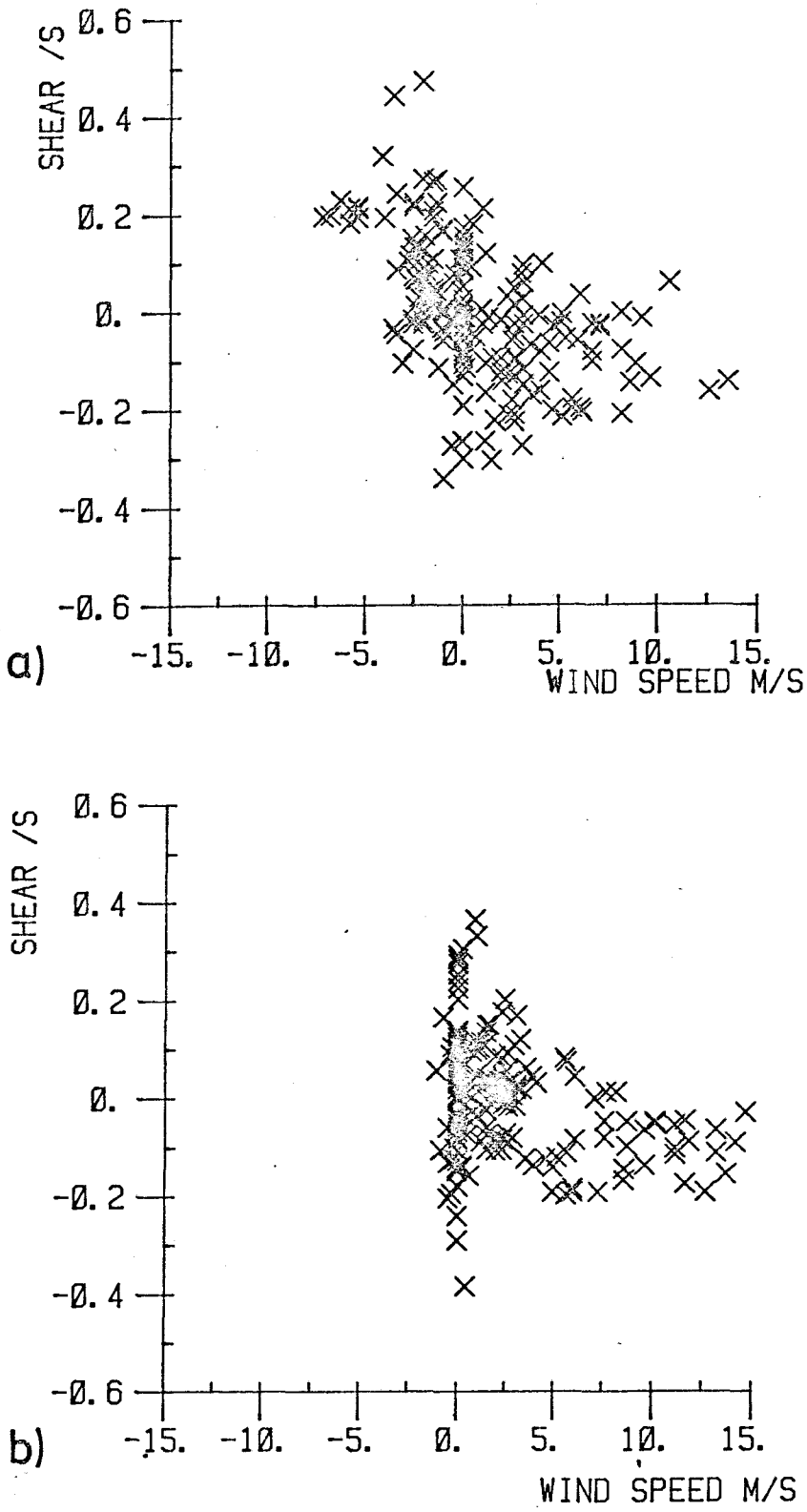

Fig. 11 Scatter plot of wind speed and current shear for 0.1 m-0.4 m.
(a) East component.
(b) North component.

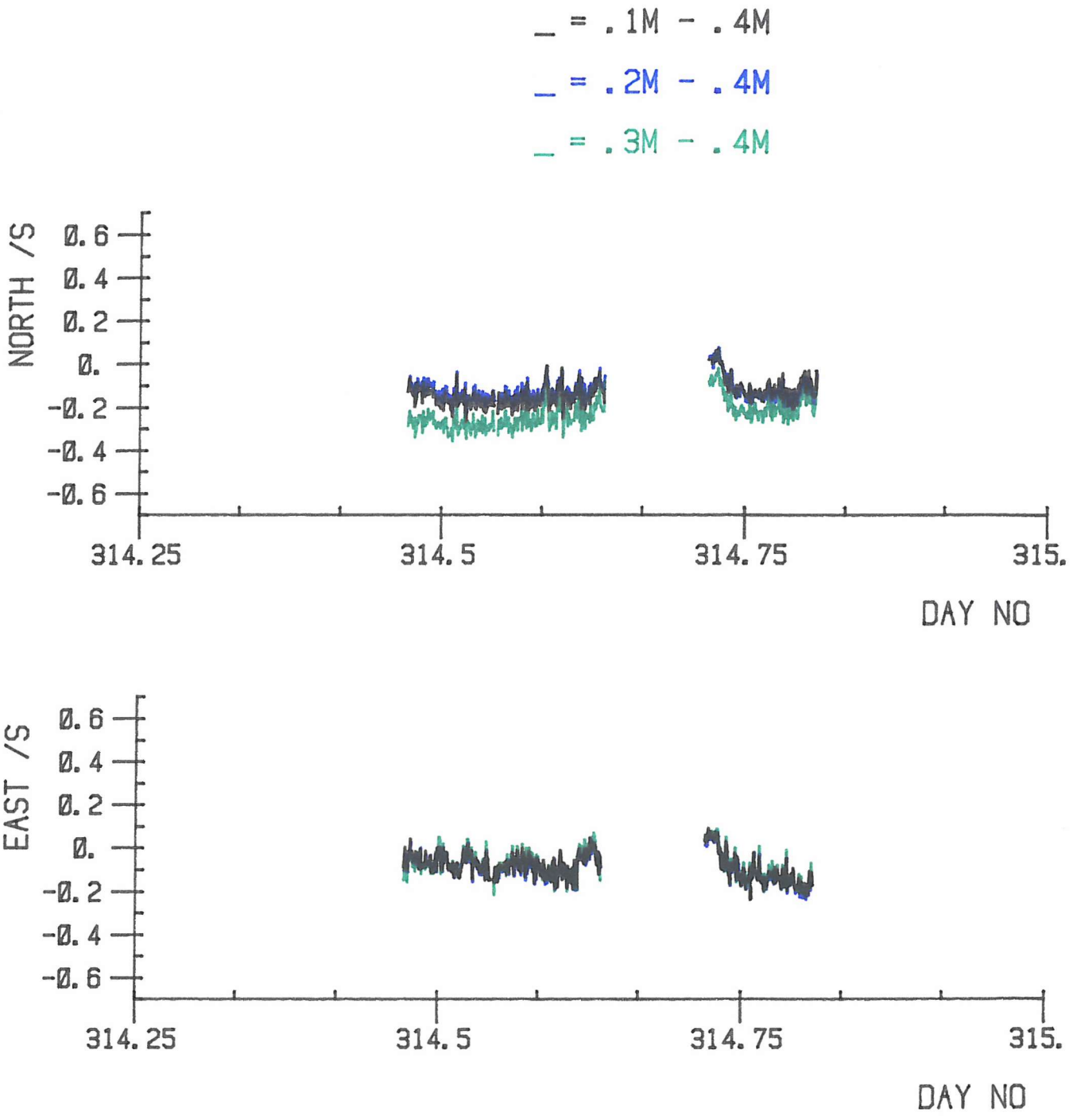

Fig. 12 Shear from the multilevel sensor for day 314.

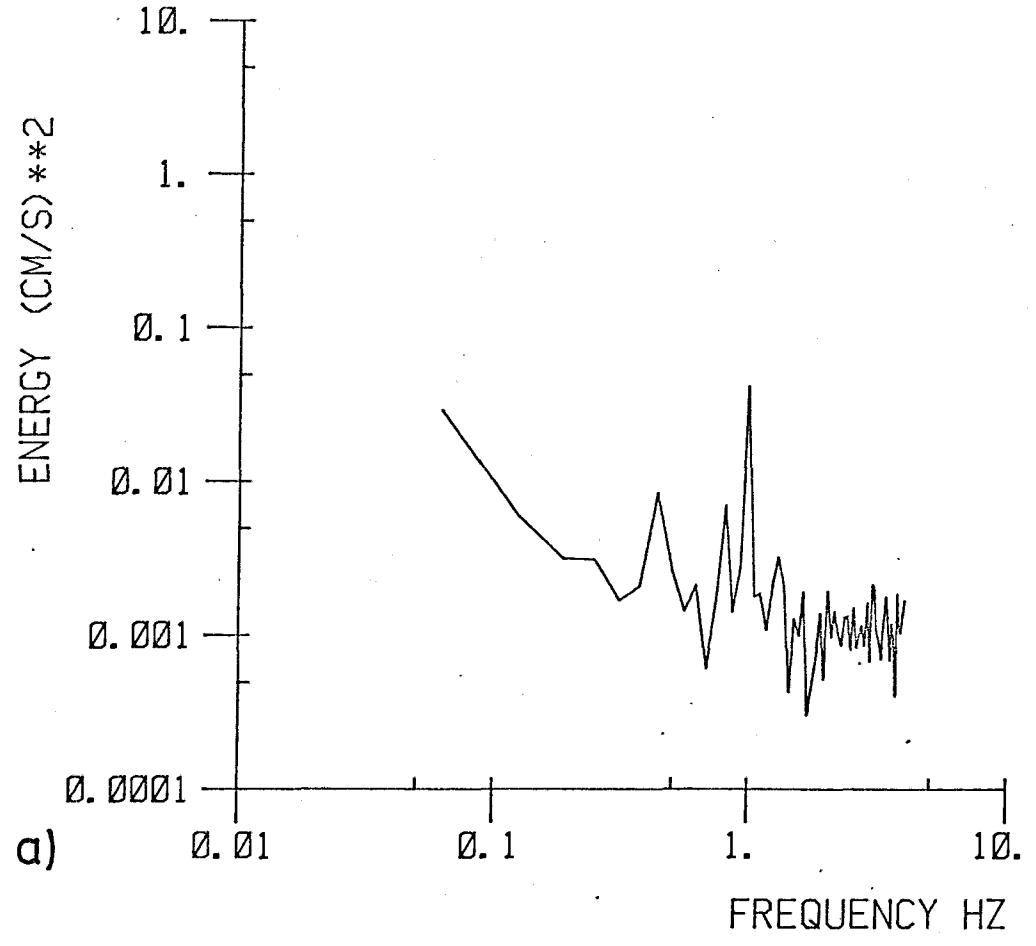

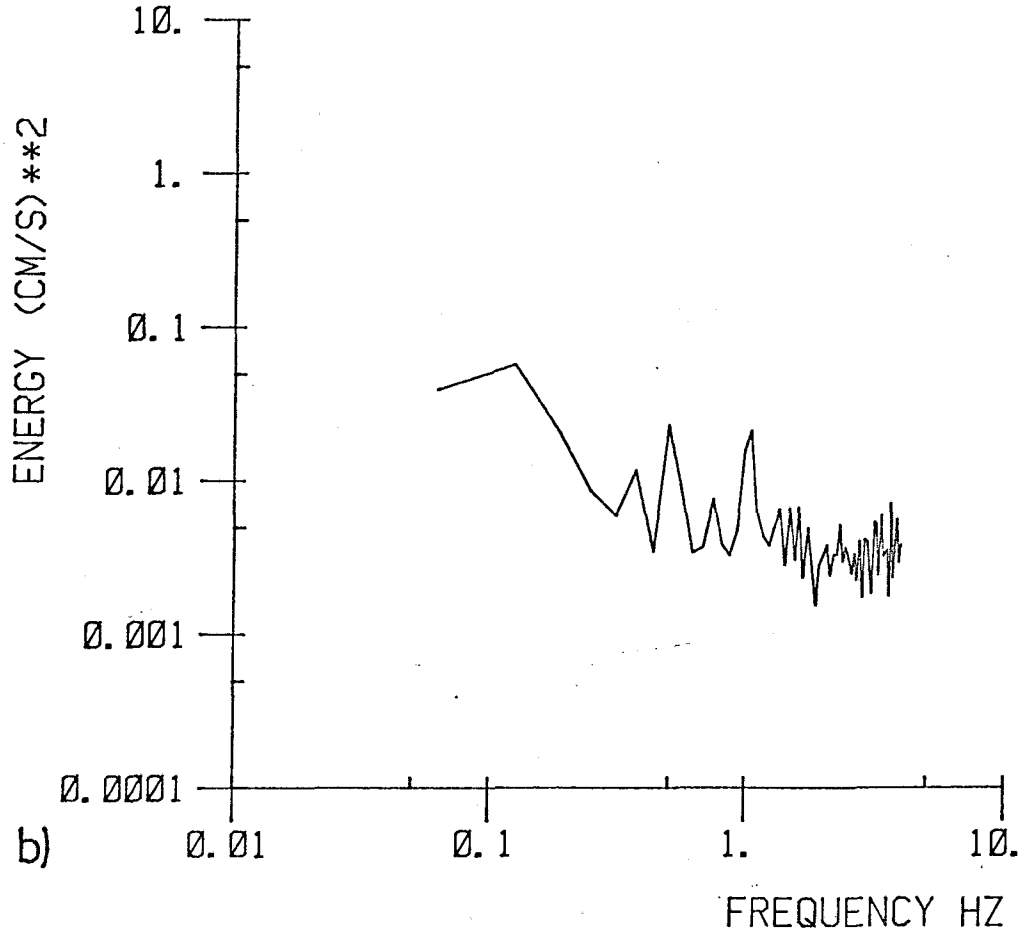

Fig. A1 Spectra of current fluctuations observed in the wavetank under steady tow at 0.4 m depth, (a) speed = 10 cm s^{-1}, (b) speed = 42 cm s^{-1}.